



## Enhanced chemosensing of ammonia based on the novel molecular semiconductor-doped insulator (MSDI) heterojunctions

Yanli Chen<sup>a</sup>, Marcel Bouvet<sup>a,\*</sup>, Thibaut Sizun<sup>a</sup>, Guillaume Barochi<sup>a,b</sup>, Jérôme Rossignol<sup>b</sup>, Eric Lesniewska<sup>b</sup>

<sup>a</sup> Institut de Chimie Moléculaire de l'Université de Bourgogne, CNRS UMR 5260, University of Bourgogne, 21078 Dijon, France

<sup>b</sup> Laboratoire Interdisciplinaire, Carnot de Bourgogne, CNRS UMR 5209, University of Bourgogne, 21078 Dijon, France

### ARTICLE INFO

#### Article history:

Received 17 August 2010

Received in revised form 28 October 2010

Accepted 22 November 2010

Available online 26 November 2010

#### Keywords:

Molecular semiconductor

Triple-decker rare earth phthalocyanine complex

Heterojunction

Chemosensing

Ammonia

### ABSTRACT

A series of new molecular semiconductor-doped insulator (MSDI) heterojunctions as conductometric transducers to NH<sub>3</sub> sensing were fabricated based on a novel semiconducting molecular material, an amphiphilic tris(phthalocyaninato) rare earth triple-decker complex, Eu<sub>2</sub>[Pc(15C5)<sub>4</sub>]<sub>2</sub>[Pc(OC<sub>10</sub>H<sub>21</sub>)<sub>8</sub>], quasi-Langmuir–Shäfer (QLS) film, as a top-layer, and vacuum-deposited and cast film of CuPc as well as copper tetra-tert-butyl phthalocyanine (CuTTBPc) QLS film as a sub-layer, named as MSDIs **1**, **2** and **3**, respectively. MSDIs **1–3** and respective sub-layers prepared from three different methods were characterized by X-ray diffraction, electronic absorption spectra and current–voltage (*I*–*V*) measurements. Depending on the sub-layer film-forming method used, α-phase CuPc film structure, β-phase CuPc crystallites and H-type aggregates of CuTTBPc have been obtained, respectively. An increasing sensitivity to NH<sub>3</sub> at varied concentrations in the range of 15–800 ppm, follows the order MSDI **2** < MSDI **3** < MSDI **1**, revealing the effect of sub-layer film structures on sensing performance of the MSDIs. In particular, the time-dependent current plot of the MSDI **1**, with α-phase CuPc film as a sub-layer, clearly shows an excellent separation of the different ammonia concentration levels and nearly complete reversibility and reproducibility even at room temperature, which is unique among the phthalocyanine-based ammonia sensors thus far reported in the literature. This provides a general method to improve sensor response of organic heterojunctions by controlling and tuning the film structure of sub-layer with appropriate fabrication techniques. On the other hand, the enhanced sensitivity, stability and reproducible response of the MSDI **1** heterostructure in comparison with the respective single-layer films have also been obtained. A judicious combination of materials and molecular architectures has led to enhanced sensing properties of the MSDI **1**, in which control at the molecular level can be achieved.

© 2010 Elsevier B.V. All rights reserved.

### 1. Introduction

The development of chemical sensors is nowadays one of the most representative examples of multidisciplinary research. The contribution of chemistry becomes critical when the aim deals with the accomplishment of better sensing performances, either from the molecular engineering of the sensitive compounds, during their assembly in solid phases or even in the final step, the device's design [1]. As the typical representative of functional molecular materials with large conjugated electronic structure, phthalocyanines offer a large variation of molecular properties, due to the great number of possible peripheral substituents and coordinated metals [2]. That versatility appears particularly on the energy levels position, their electrochemical properties and their intermolecular interactions, for example with adsorbed gaseous

molecules [3]. Thus, phthalocyanines behave either as semiconductor or as doped insulator (extrinsic semiconductors, of n- or p-type, depending on their chemical nature) [1]. The modulation of the electrical properties of these materials by exposure to oxidizing or reducing gases is known to arise from their semiconductor behavior [4–6]. While neat metallophthalocyanine thin films can, under controlled conditions, function as responsive chemiresistors, they have important operational drawbacks as standalone sensors. Metallophthalocyanines generally require both a high temperature (80–170 °C) as well as a large applied electric field to function as chemiresistors [7,8]. Among the large family of the phthalocyanines, double-decker phthalocyanines, and especially the lutetium derivatives, have been subject to extensive investigations because of their radical nature and their possible use in gas sensing applications as well as in photovoltaic and organic electronic devices [9,10]. On the other hand, tetrapyrrole rare earth triple-decker analogues have aroused increasing attention because of the extension of the π networks along the axis perpendicular to the macrocycle plane [11–13]. Solution-processed thin solid films

\* Corresponding author. Tel.: +33 380396086; fax: +33 380396098.

E-mail address: [marcel.bouvet@u-bourgogne.fr](mailto:marcel.bouvet@u-bourgogne.fr) (M. Bouvet).

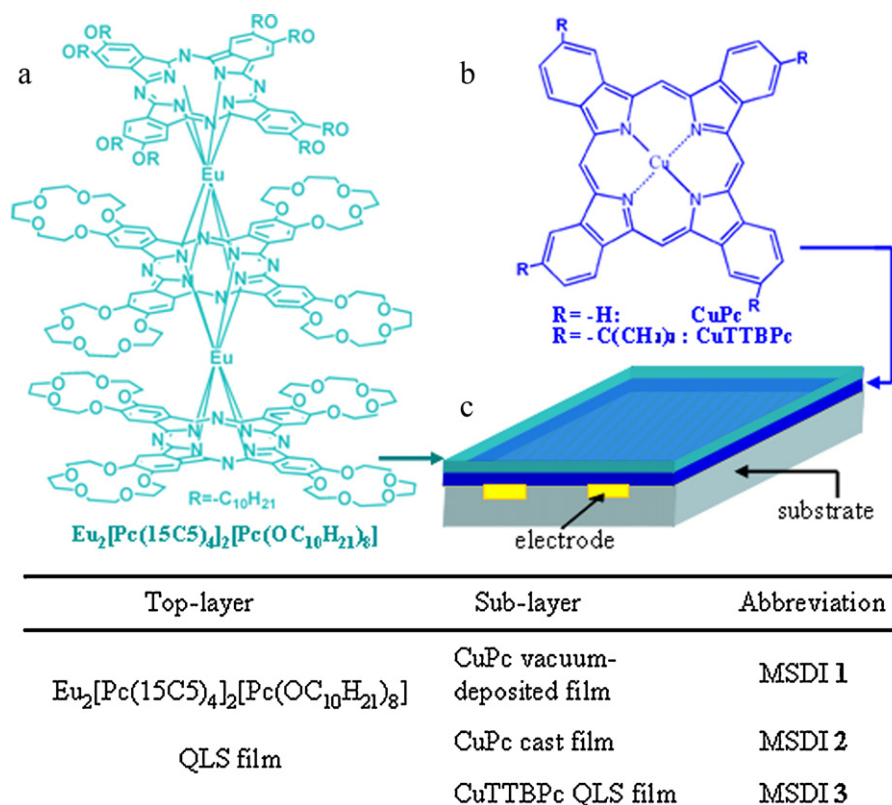


Fig. 1. Schematic molecular structures as (a) top-layer, (b) sub-layer of the MSDI and (c) architecture of the MSDI device.

of amphiphilic tris(phthalocyaninato) rare earth triple-deckers  $\text{M}_2[\text{Pc}(\text{15C5})_4]_2[\text{Pc}(\text{OC}_8\text{H}_{17})_8]$  ( $\text{M} = \text{Eu}, \text{Tb}, \text{Lu}$ ) have been revealed to display excellent FET performance [14]. This led to the synthesis, characterization, and systematic investigation for the semiconductor properties of a series of amphiphilic tris(phthalocyaninato) rare earth triple-decker complexes [15–18].

In previous work, we designed and characterized a new type of conductimetric transducer, called MSDI for molecular semiconductor-doped insulator heterojunction and resulting from the combination of two types of molecular materials [19]. It is a simple device formed by a thin film-based heterostructure. We used as a sub-layer with diverse functional molecular materials, such as unsubstituted or fluorinated copper phthalocyanine  $\text{Cu}(\text{F}_n\text{Pc})$  ( $n = 0, 8, 16$ ), which is in contact with two interdigitated electrodes by vacuum sublimation, and vacuum-deposited  $\text{LuPc}_2$  film as a top layer, being the only material available to interact with the outer atmosphere. In the MSDI heterojunction, due to its own electronic properties, the gas sensitivity of  $\text{LuPc}_2$  was modulated, even inverted, depending on the nature of the doped insulator used as sub-layer [20,21]. Very recently, we developed successfully a simple quasi-Langmuir–Shäfer (QLS) process for fabricating ordered ultra-thin films of an amphiphilic tris(phthalocyaninato) rare earth triple-decker complex,  $\text{Eu}_2[\text{Pc}(\text{15C5})_4]_2[\text{Pc}(\text{OC}_{10}\text{H}_{21})_8]$ , as chemiresistive  $\text{O}_3$  sensor. Sensitive, stable and reproducible responses to  $\text{O}_3$  gas were obtained for this kind of ultra-thin QLS films [22]. However, such examples for triple-decker phthalocyanines-based sensors are still rare. In the present work, we prepare a series of new MSDI heterojunctions as conductimetric transducers to  $\text{NH}_3$  sensing based on  $\text{Eu}_2[\text{Pc}(\text{15C5})_4]_2[\text{Pc}(\text{OC}_{10}\text{H}_{21})_8]$  QLS film as a top-layer, and vacuum-deposited and cast film of CuPc as well as copper tert-butyl phthalocyanine (abbreviated as CuTTBPc) QLS film as a sub-layer, named as MSDIs 1, 2 and 3, respectively (Fig. 1). MSDIs 1–3 and respective sub-layers prepared from three differ-

ent methods were characterized by X-ray diffraction, electronic absorption spectra and current–voltage ( $I$ – $V$ ) measurements. The gas-sensing characteristics exhibit a strong dependence on the film structure of sub-layer, which provides a general method to improve sensor response of organic heterojunctions by controlling and tuning the film structure of sub-layer with appropriate fabrication techniques. Furthermore, the enhanced sensitivity, stability and reproducible response of the MSDI 1 heterostructure in comparison with the respective single-layer film have also been obtained. The present work, representing our continuous efforts in understanding the relationship between the film structure and gas sensor performance of tetrapyrrole organic semiconductors [19–22], will be helpful for attracting further research interests over the new transducer in the field of chemical sensors and the semiconducting properties of phthalocyanine derivatives, in particular triple-decker rare earth phthalocyanines for sensor applications.

## 2. Experimental

### 2.1. Materials and chemicals

CuPc ( $\beta$ -phase) and CuTTBPc were purchased from Aldrich Chem. Co. (purity: 97%) and used without further purification. The amphiphilic heteroleptic tris(phthalocyaninato) rare earth triple-decker complex,  $\text{Eu}_2[\text{Pc}(\text{15C5})_4]_2[\text{Pc}(\text{OC}_{10}\text{H}_{21})_8]$ , was used as synthesized previously [16]. All other reagents and solvents were of reagent grade and used as received.

### 2.2. Devices fabrication

The heterojunctions as MSDI devices were built by two-step deposition of the corresponding molecular materials onto ITO/glass interdigitated electrodes (IDEs), which contained 10 pairs of ITO electrode fingers deposited onto a glass substrate, separated by

75  $\mu\text{m}$  with 20 nm electrode thickness. Firstly, vacuum-deposited and cast films of CuPc as well as CuTTBPc QLS film, as a sub-layer of MSDIs **1**, **2** and **3**, respectively, were fabricated. And then  $\text{Eu}_2[\text{Pc}(\text{15C5})_4]_2[\text{Pc}(\text{OC}_{10}\text{H}_{21})_8]$  as the top layer was transferred on sub-layer of three types of MSDI devices by the QLS technique, respectively [22].

Thin film deposition was conducted as following: (i) *vacuum-deposited CuPc film*: the 100 nm thick film of CuPc was deposited on ITO/glass IDEs by means of classical thermal evaporation (using a VEECO 770 system) from a tantalum boat, at ca.  $10^{-6}$  mbar, and a  $2 \text{ \AA s}^{-1}$  rate. Deposition rate and film thickness were monitored by quartz crystal microbalance; (ii) *cast film*: due to the poor solubility in organic solvent, CuPc powder was dispersed ultrasonically in chloroform ( $4.1 \text{ mg mL}^{-1}$ ). 20  $\mu\text{L}$  of CuPc suspension was cast on an ITO/glass IDEs ( $1 \text{ cm} \times 1 \text{ cm}$ ), using a glass micro-syringe and thus subject to drying in air. The thickness of resulting films was estimated to about 500 nm (CuPc density:  $1.62 \text{ g cm}^{-3}$ ); (iii) *quasi-Langmuir–Shäfer (QLS) film*: QLS film was prepared as described previously [22]. Briefly, 4.0 mL of CuTTBPc ( $0.31 \text{ mg mL}^{-1}$ ,  $4.5 \times 10^{-4} \text{ mol L}^{-1}$ ) and  $\text{Eu}_2[\text{Pc}(\text{15C5})_4]_2[\text{Pc}(\text{OC}_{10}\text{H}_{21})_8]$  ( $0.30 \text{ mg mL}^{-1}$ ,  $6.5 \times 10^{-5} \text{ mol L}^{-1}$ ) chloroform solution was put into a cylindrical glass container (ca.  $24 \text{ cm}^3$  internal volume), respectively, then 2 mL water was slowly added onto the surface of the solution, while chloroform solution surface of the sample was incompletely covered by water. During  $\text{CHCl}_3$  solvent evaporation, organic molecules gradually assembled to form some fine nanostructures at the  $\text{CHCl}_3$ /water interface. After complete evaporation of  $\text{CHCl}_3$ , the densely packed film remained on the water surface. After carefully adding more water into the container, the film can be easily transferred by horizontal lifting from the water surface onto the ITO/glass IDEs. The process was repeated to obtain the required number of layers. Residual water on the substrates, between transfer steps and after the final transfer, was removed with a stream of argon. It should be noted that, prior to the deposition, substrates were successively sonicated in dichloromethane, methanol and distilled water and dried with argon gas. In present case, the 15-layer CuTTBPc and 6-layer  $\text{Eu}_2[\text{Pc}(\text{15C5})_4]_2[\text{Pc}(\text{OC}_{10}\text{H}_{21})_8]$  QLS film are obtained as sub-layer of MSDI **3** and top-layer of all MSDIs, respectively.

### 2.3. Characterization

X-ray diffraction (XRD) experiments were carried out on Goniometric CPS 120/Cu X-ray diffractometer with copper ( $K\alpha$ ) radiation ( $\lambda = 1.5406 \text{ \AA}$ ). UV–vis absorption spectra were recorded on a Varian Cary/1E UV–visible spectrophotometer. A bare ITO/glass IDE was used as a reference for UV–vis spectra measurement. Atomic force microscopy (AFM) images were collected in air under ambient conditions using the tapping mode with a Veeco Nanoscope Multimode IIIA SPM.

### 2.4. Device measurements

The fundamental electrical and sensor measurements were performed using a Keithley 6517 electrometer with an incorporated DC voltage supply, always at room temperature. The electrometer is controlled by self-made software via the GP-IB board. Current–voltage ( $I$ – $V$ ) curves were registered in the range ( $-10$  and  $+10 \text{ V}$ ), starting and finishing at  $0 \text{ V}$  bias to avoid irreversible polarization effects. On the other hand, the  $\text{NH}_3$ -sensing properties of samples have been examined by exposing the corresponding films to different concentrations of ammonia and measuring the current changes of the films at a constantly polarized voltage of  $5 \text{ V}$ .

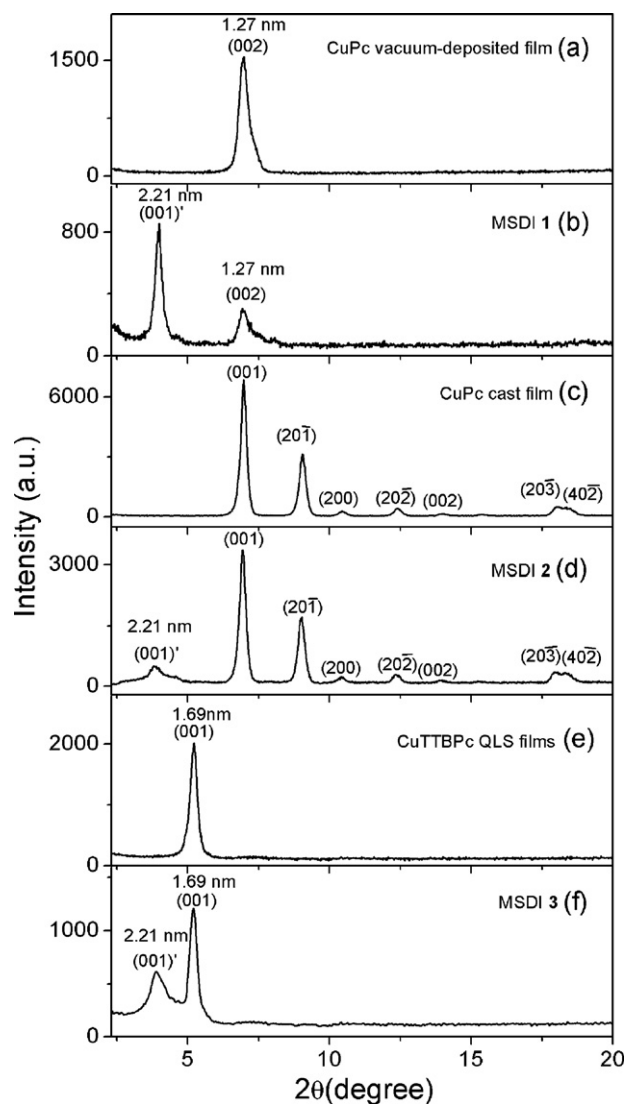


**Fig. 2.** X-ray diffraction patterns of the sub-layer and corresponding MSDI heterojunction on ITO/glass IDEs: (a) CuPc vacuum-deposited film, (b) MSDI **1**, (c) CuPc cast film, (d) MSDI **2**, (e) CuTTBPc QLS film, and (f) MSDI **3**.

### 2.5. Gas sources for sensing experiments

The desired ammonia concentration was produced by diluting a mixture  $\text{NH}_3/\text{Ar}$  (1000 ppm  $\text{NH}_3$ , from Air Liquide, France) with dry Ar using two mass flow controllers (total mass flow:  $0.5 \text{ L min}^{-1}$ ). The maximum water contents in ammonia and argon cylinders purchased were 100 ppm and 2 ppm respectively.

## 3. Results and discussion

### 3.1. XRD study

The quality of the three types of MSDI film and corresponding sub-layers has been assessed using X-ray diffraction (XRD) technique. The MSDIs **1–3** and corresponding sub-layers deposited on ITO/glass IDEs give clear diffraction peaks (Fig. 2). The XRD diagram of a vacuum-deposited CuPc film shows only one well-defined diffraction peak at  $2\theta = 6.97^\circ$  ( $d = 1.27 \text{ nm}$ ) (Fig. 2a). The distance of 1.27 nm between the plane of the copper atoms in one layer and that in the next layer is in fair agreement with the reference value (1.26 nm) of the  $\alpha$ -phase CuPc [23,24]. The single peak is the result of diffraction from the (002) lattice planes

of  $\alpha$ -phase CuPc separated by approximately the inter-stacking distance [25,26], therefore, implies that the trace of the herringbone pattern is parallel to the substrate, which is confirmed by the UV–vis experimental result as detailed below. The XRD pattern of MSDI 1 heterojunction is shown in Fig. 2b. It consists of two different peaks at  $2\theta = 3.98^\circ$  ( $d = 2.21$  nm),  $6.97^\circ$  ( $d = 1.27$  nm), corresponding to the (001) and (002) lattice plane of the top-layer and sub-layer, respectively [22–24]. The (001) Bragg diffraction peak of  $\text{Eu}_2[\text{Pc}(15\text{C}5)_4]_2[\text{Pc}(\text{OC}_{10}\text{H}_{21})_8]$  QLS film as a top-layer appeared in MSDI 1 heterojunction indicates the existence of an ordered layer structure parallel to the substrate [22,27,28]. The typical amphiphilic properties of the triple-decker molecule ensure the high quality of the multilayer film fabricated by a simple QLS thin-film deposition technique. According to our previous studies [22], the  $d$ -spacing of 2.21 nm is assigned to the distance between two adjacent  $\text{Eu}_2[\text{Pc}(15\text{C}5)_4]_2[\text{Pc}(\text{OC}_{10}\text{H}_{21})_8]$  molecules in the longitudinal direction, in which  $\text{Eu}_2[\text{Pc}(15\text{C}5)_4]_2[\text{Pc}(\text{OC}_{10}\text{H}_{21})_8]$  molecules took a face-on conformation with edge-to-edge stacking. Furthermore, the diffraction peak of a vacuum-deposited CuPc film in both MSDI 1 and its single-layer film has the same position, as compared in Fig. 2a and b, implying that CuPc molecules in MSDI 1 heterojunction still took the same molecular stacking structures as in the single-layer film. Therefore, the configuration on the CuPc planes is oriented edge on with respect to the substrate, which is believed to be favorable in charge-carrier transportation at the interface of the two phases [26]. On the other hand, X-ray diffraction pattern of CuPc cast film shown in Fig. 2c is analogous to the powder diffraction pattern reported for  $\beta$ -CuPc in the literature [29]. Indexing was carried out for seven peaks in the lower angle part (less than  $20^\circ$  in  $2\theta$ ), labeled in Fig. 2c and d, which is known to be a thermally stable  $\beta$ -phase polymorph of CuPc and its structure was found by Brown to have a monoclinic  $P2_1/a$  space group [29]. The observation of a number of peaks at a low angle region indicates that the CuPc cast film in the present case ( $\approx 500$ -nm thick) consists of randomly oriented  $\beta$ -CuPc crystallites in this case.

Due to its poor solubility, it was impossible to deposit CuPc film by the QLS technique. It is the reason why CuTTBPc was chosen as sub-layer of MSDI 3 in order to take advantage of the QLS technique. A Bragg diffraction peak of CuTTBPc QLS film occurred at  $2\theta = 5.22^\circ$ , which corresponds to a diffraction period of 1.69 nm as shown in Fig. 2e. The peak position is almost the same as in CuTTBPc LB film ( $2\theta = 5.29^\circ$ ,  $d = 1.67$  nm) reported by Lee et al. [30]. From this literature, CuTTBPc molecules in its LB films fabricated by vertical deposition took a face-to-face configuration with their molecular planes perpendicular and the molecular columns parallel to the substrate surface. Therefore, it can be deduced that CuTTBPc molecules have here a similar face-to-face configuration. It should be noted that two group diffraction peaks were also obtained in both MSDI 2 and MSDI 3 heterojunctions (Fig. 2d and f), which belong to  $\text{Eu}_2[\text{Pc}(15\text{C}5)_4]_2[\text{Pc}(\text{OC}_{10}\text{H}_{21})_8]$  QLS film (as the top-layer) and CuPc cast film or CuTTBPc QLS film (as the sub-layer), respectively. However, the peak position of  $\text{Eu}_2[\text{Pc}(15\text{C}5)_4]_2[\text{Pc}(\text{OC}_{10}\text{H}_{21})_8]$  QLS film in MSDIs 1–3 did not show a significant change (Fig. 2b, d, and f), suggesting similar packing behavior of the  $\text{Eu}_2[\text{Pc}(15\text{C}5)_4]_2[\text{Pc}(\text{OC}_{10}\text{H}_{21})_8]$  molecules deposited onto the three different types of sub-layer.

### 3.2. UV–vis absorption spectra

To further obtain information about the films structures, UV–vis absorption spectra of the MSDIs 1–3 and the corresponding sub-layer deposited on ITO/glass IDEs were recorded as shown in Fig. 3. In a previous work, we have already reported the electronic absorption spectrum of the  $\text{Eu}_2[\text{Pc}(15\text{C}5)_4]_2[\text{Pc}(\text{OC}_{10}\text{H}_{21})_8]$  QLS film [22]. It displays a broadened and red-shifted Q-band (654 nm), as compared to that in solution (647 nm) due to formation of edge-

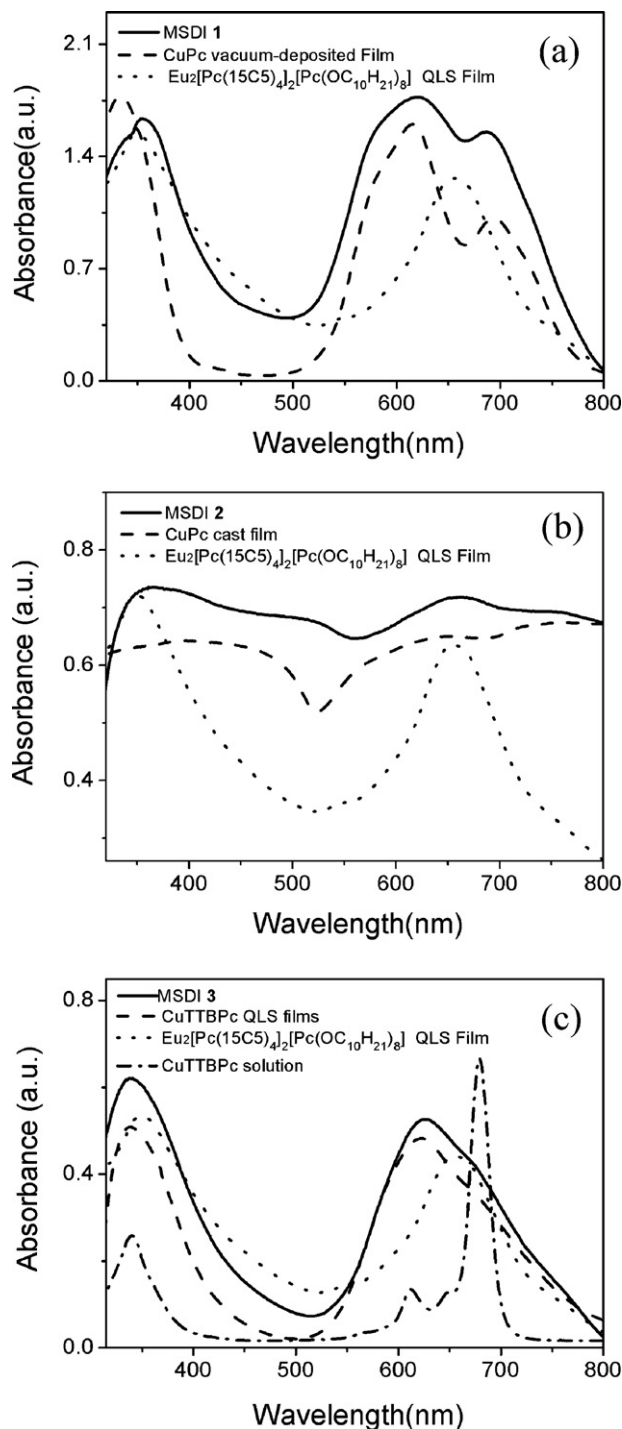


**Fig. 3.** UV–vis absorption spectra of the MSDI heterojunction (solid line) compared to corresponding sub-layer (dashed line) and top-layer (dotted line) on ITO/glass IDEs. (a) MSDI 1 and the respective single-layer films, (b) MSDI 2 and the respective single-layer films, (c) MSDI 3 and the respective single-layer films as well as CuTTBPc in  $\text{CHCl}_3$  (dashed dotted line).

to-edge-type aggregates (J-type aggregates), which is also shown in Fig. 3 (dotted line) for comparison purposes. It has been suggested that the UV–vis spectrum of MPCs originates from the molecular orbitals within the aromatic  $18-\pi$  electron system and from overlapping orbitals on the central metal [31]. It is seen that for the vacuum-deposited CuPc film (Fig. 3a, dashed line), absorption due to  $\pi-\pi^*$  transitions on the phthalocyanine macrocycle appeared in the visible region at 616 and 694 nm (Q band) exhibiting a doublet

due to Davydov splitting [32–35]. And the intensity of the higher energy (616 nm) peak is larger than that of the lower energy peak (694 nm). This represents a typical feature of  $\alpha$ -CuPc [24]. Furthermore, the Q band of the vacuum-deposited CuPc film is broadened and blue shifted with respect to that of CuPc in solution reported by Lin and co-workers [32], indicating the formation of a face-to-face (H-type aggregates) stacked molecular structure and strong intramolecular interactions between phthalocyanine rings. These are well in accordance with the conclusion deduced from XRD studies detailed above. For CuPc cast film (Fig. 3b, dashed line), peaks are shifted to 640 and 715 nm and the intensity of the higher energy peak is smaller than that of the lower energy peak indicating the formation of  $\beta$ -CuPc [24,31,36], in agreement with XRD results. Solution and thin film absorbance spectra of CuTTBPC are shown in Fig. 3c. The dilute chloroform solutions of CuTTBPC show Q-band absorbance at ca. 679 nm (Fig. 3c, dashed dotted line), corresponding to the Pc monomer [30]. With CuTTBPC QLS film, the Q-band broadens and blue-shifts to yield a peak at ca. 622 nm, which arises from co-facial aggregation of the Pc [30,37], also consistent with XRD results.

For MSDIs 1–3, the UV–vis spectra show the absorption characteristics of both a top-layer ( $\text{Eu}_2[\text{Pc}(15\text{C}5)_4]_2[\text{Pc}(\text{OC}_{10}\text{H}_{21})_8]$  QLS film) and a sub-layer (CuPc or CuTTBPC film), shown in Fig. 3a–c (solid line), hinting at the presence of a segregated molecular stacking structure. UV–vis spectrum of MSDI 1 shows the distinct characterized two Q-bands, appearing in the region between 550 and 750 nm, in Fig. 3a, solid line. Since the Q-bands of both  $\text{Eu}_2[\text{Pc}(15\text{C}5)_4]_2[\text{Pc}(\text{OC}_{10}\text{H}_{21})_8]$  QLS film (654 nm) and  $\alpha$ -CuPc film lie in the same region, the overlap of Q-band from top-layer and sub-layer results in broaden Q-band at 623 and 686 nm, respectively. Obviously, a doublet due to Davydov splitting from  $\alpha$ -CuPc film still exists in MSDI 1 heterojunction. For UV–vis spectrum of MSDI 2 (Fig. 3b, solid line), the two relative intense absorption bands, at around 656 and 350 nm, correspond to the Q-band and B-band of  $\text{Eu}_2[\text{Pc}(15\text{C}5)_4]_2[\text{Pc}(\text{OC}_{10}\text{H}_{21})_8]$  QLS film, respectively. And the character of Davydov splitting of Q-band from  $\beta$ -CuPc film is also present in the heterojunction, compared to single-layer film of  $\beta$ -CuPc (Fig. 3b, dashed line). The spectrum of the MSDI 3 exhibits a main Q-bands at 626 and a shoulder near 660 nm, which belongs to CuTTBPC and  $\text{Eu}_2[\text{Pc}(15\text{C}5)_4]_2[\text{Pc}(\text{OC}_{10}\text{H}_{21})_8]$  QLS film, respectively.

### 3.3. Current–voltage (*I*–*V*) characteristics

To ensure that all the devices, MSDIs 1–3 and the respective single-layer films, have a good electrical contact to the electrodes, the *I*–*V* curves were measured. All devices exhibit similar Ohmic behavior at low bias voltages, shown in Fig. 4. In the MSDI devices, the positive and negative polarizations correspond to charge injection in the CuPc sub-layer, in contrast to the typical forward and reverse polarizations in diode-type heterojunctions [20,21]. As a result, the current developed by the MSDIs remains perfectly symmetrical. However, the response increases in the order MSDI 2 (current amplitude in the  $9.3 \times 10^{-8}$  A range) < MSDI 3 (current amplitude in the  $2.5 \times 10^{-7}$  A range) < MSDI 1 (current amplitude in the  $3.7 \times 10^{-7}$  A range). A very similar trend of current change is also observed in the respective sub-layer of MSDIs 1–3: CuPc cast film (as a sub-layer of MSDI 2, current amplitude in the  $3.9 \times 10^{-9}$  A range) < CuTTBPC QLS film (as a sub-layer of MSDI 3, current amplitude in the  $5.0 \times 10^{-9}$  A range) < CuPc vacuum-deposited film (as a sub-layer of MSDI 1, current amplitude in the  $4.8 \times 10^{-8}$  A range). Thus, there is a significant sub-layer film structure dependence for the conductivity of semiconducting MSDI 1–3. In light of the previous observations, and as reported in the literature with regard to electrical characterization of MPcs compounds [14,15,17,18,22,25,28]: higher is the order of a one-dimensional densely packed molecular architecture in the film matrix, higher is

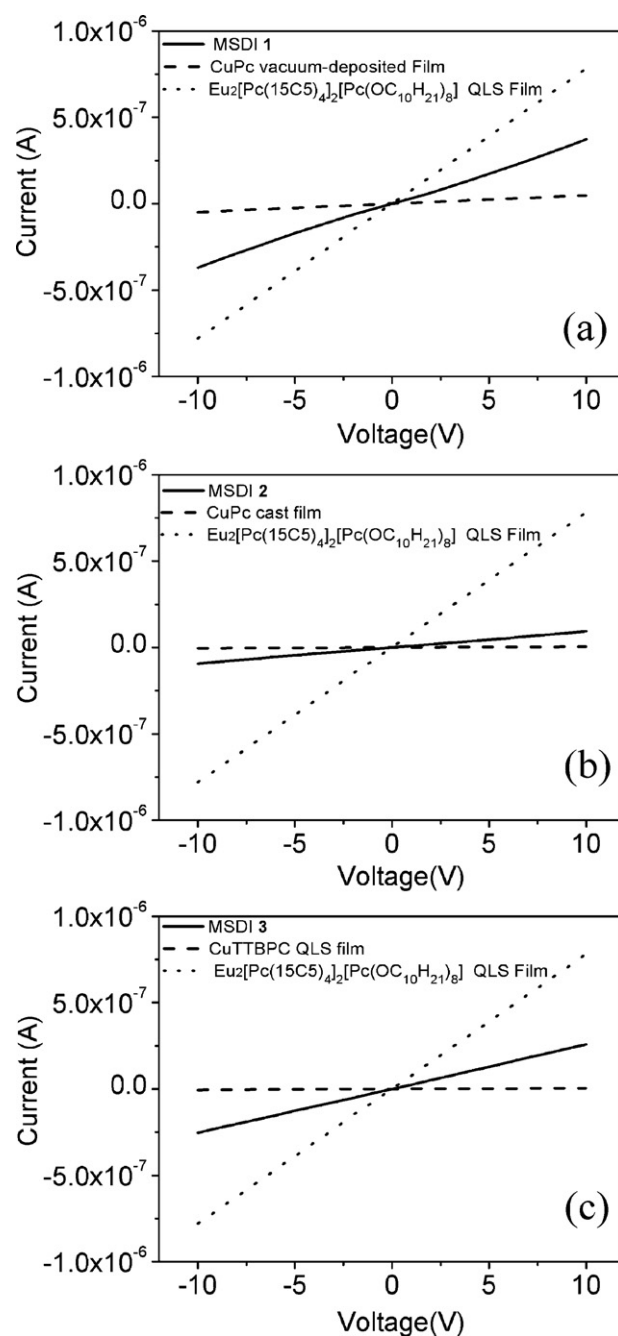
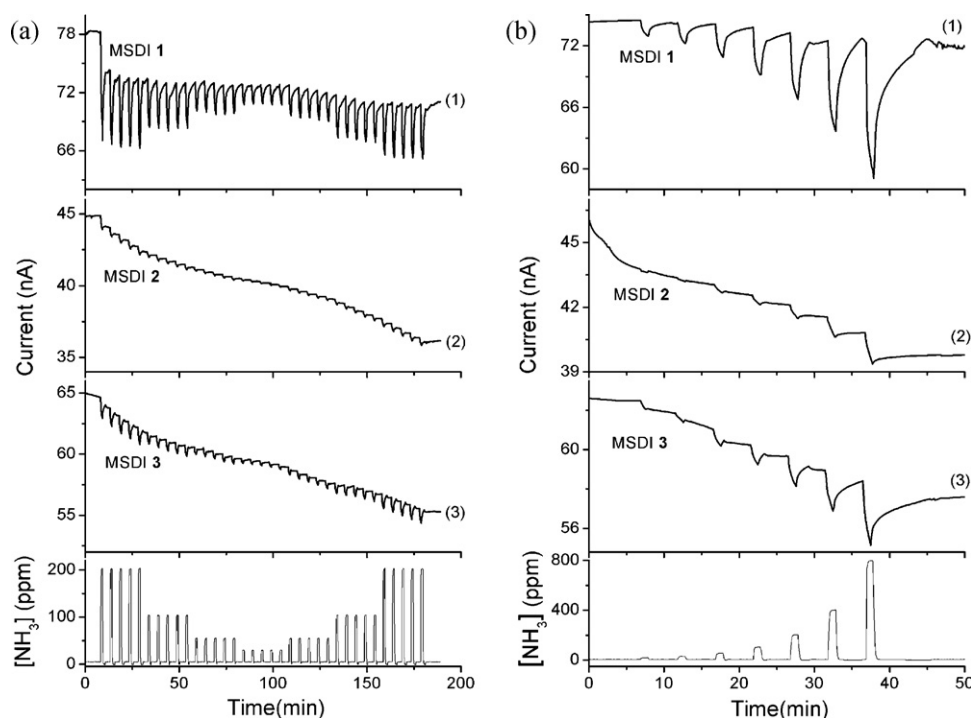


Fig. 4. Representative *I*–*V* characteristics of (a) MSDI 1 and the respective single-layer films, (b) MSDI 2 and the respective single-layer films, and (c) MSDI 3 and the respective single-layer films.

the mobility of charge carriers, resulting in a higher current passed through the devices. For the  $\beta$ -CuPc, continuity of the conductive path is disrupted by the randomly oriented  $\beta$ -CuPc crystallites, having little contributions to the conductivity [5], thus the current is much smaller than that of the  $\alpha$ -CuPc films. So, the best film quality of sub-layer of these MSDIs has been obtained by vacuum sublimation of CuPc in MSDI 1. In any case, the current developed by MSDI heterojunctions is higher than that exhibited by doped insulator single layer resistors (current amplitude in the  $5 \times 10^{-8}$  to  $4 \times 10^{-9}$  A range), but lower than that developed by  $\text{Eu}_2[\text{Pc}(15\text{C}5)_4]_2[\text{Pc}(\text{OC}_{10}\text{H}_{21})_8]$  single layer (current amplitude in the  $8 \times 10^{-7}$  A range). This indicates that the charge transfer in the MSDI heterostructures is governed by both the charge injec-



**Fig. 5.** The time-dependent current plots for MSDIs 1–3 exposed to different ammonia concentrations for 1 min exposure and 4 min recovery period in the range of (a) 50–200 ppm, and (b) 15–800 ppm, while the bottom rectangular pulses for each current plot represent the  $\text{NH}_3$  concentration as a function of time.

tion into the sub-layer and the current flowing across the organic heterointerface. Instead of the determined conductivity of single semiconductor layer, the conductivity of the bilayer device is tuned by changing film forming method of sub-layers.

Before gas sensing measurement, the stability of current of MSDIs 1–3, and corresponding sub-layer as well as  $\text{Eu}_2[\text{Pc}(15\text{C}5)_4]_2[\text{Pc}(\text{OC}_{10}\text{H}_{21})_8]$  film, in dry argon (as diluent gas for different concentrations of  $\text{NH}_3$ , total mass flow:  $0.5 \text{ L min}^{-1}$ ), has been tested by a  $I$ - $V$  measurement in the range ( $-10$  and  $+10\text{V}$ ) for the continuous 20 cycles, starting and finishing at  $0\text{V}$  bias. The current of the devices showed a relative stable behavior vs. time. Fig. A1 (Suppl. Mater.) displays the time-dependent current plots of MSDI 1, CuPc vacuum-deposited film and the  $\text{Eu}_2[\text{Pc}(15\text{C}5)_4]_2[\text{Pc}(\text{OC}_{10}\text{H}_{21})_8]$  QLS film exposed to dry argon, in the range ( $-10$  and  $+10\text{V}$ ), as typical examples of the MSDI and sub-layer series, together with that of the  $\text{Eu}_2[\text{Pc}(15\text{C}5)_4]_2[\text{Pc}(\text{OC}_{10}\text{H}_{21})_8]$  QLS film (as a top-layer). So, the effect of the value of relative humidity on the surrounding atmosphere on the  $\text{NH}_3$  response properties was neglected in the present case. The combined effect of ammonia and water has been reported previously with  $\text{LuPc}_2$  resistors [10].

### 3.4. Responses of the devices to $\text{NH}_3$

Responses of the MSDIs 1–3 sensors were determined from the time-dependent current plots when exposed to  $\text{NH}_3$  (15–800 ppm) diluted in dry argon, at room temperature. The sensing performances were studied with a duty cycle where dynamic exposure period is fixed at 1 min and static recovery period at 4 min. As expected (Fig. 5), current of the MSDIs 1–3 devices decreases under ammonia, due to a decrease of the density of free charge carriers in the  $\text{Eu}_2[\text{Pc}(15\text{C}5)_4]_2[\text{Pc}(\text{OC}_{10}\text{H}_{21})_8]$  layer of the MSDIs 1–3, which should be attributed to hole trapping within the p-type film by electrons donated from the chemisorbed  $\text{NH}_3$  [38,39]. It can be seen qualitatively in Fig. 5 that, the reversibility, reproducibility and response to  $\text{NH}_3$  follow the order MSDI 1 > MSDI 3 > MSDI 2, reveal-

ing the effect of sub-layer film structures on sensing performance of the MSDIs. In particular, change in current of the MSDI 1, with the CuPc vacuum-deposited film (100-nm thick) as a sub-layer, clearly shows an excellent separation of the different ammonia concentration levels and nearly complete reversibility and reproducibility after undergoing only one dynamic exposure–recovery (inert gas flow) cycle, even at room temperature (Fig. 5a(1)). The current drift at the end of the recovery period is  $0.095 \text{ nA}$  per cycle for MSDI 1, i.e.,  $0.13\%$  of start current ( $74.3 \text{ nA}$ ) for the overall experiment. This feature shows a comparatively better reversibility and reproducibility toward  $\text{NH}_3$  at room temperature as compared to both a  $\text{LuPc}_2$ /PTCDI MSDI heterojunction-based sensor tested by Bouvet et al. [21] and a polypyrrole-based amperometric ammonia sensor reported by Lähdesmäki et al. [40]. It is interesting to reveal that the ammonia gas sensor based on MSDI 1 shows a much better response in comparison to phthalocyanine-based materials like  $\text{LuPc}_2$  thin films at room temperature [10] and  $\text{ZnPc}$  at  $180^\circ\text{C}$  [39].

In order to quantitatively analyze the sensor responses, the percent current change was calculated for each concentration, as follows:

$$\% \text{current change} = \left[ \frac{I_0 - I_f}{I_0} \right] \times 100 \quad (1)$$

where  $I_0$  is the current at the start of an exposure/rest cycle and  $I_f$  is the current at the end of the 1 min exposure period. That value is designated as the sensor response. In the present case, the exact values of  $I_0$  and  $I_f$ , at a given  $\text{NH}_3$  concentration are selected from each exposure period of five repeated cycles series as depicted from Fig. 5a. The MSDIs 1–3 sensor responses are linear with respect to  $\text{NH}_3$  concentration ( $\text{Adj. } R^2 \geq 0.98$ ) (Fig. 6), suggesting first-order analyte–film interaction kinetics [41]. The slope ( $\% \text{ ppm}^{-1}$ ) of the linear fit of the percent current changes as a function of  $\text{NH}_3$  concentration, for MSDIs 1, 2 and 3 is 0.041, 0.0057 and 0.0091, respectively. The highest sensor response is obtained for the MSDI 1 with a sub-layer of 100-nm thick vacuum-deposited film of CuPc. The relative sensitivity for MSDI 3 with a

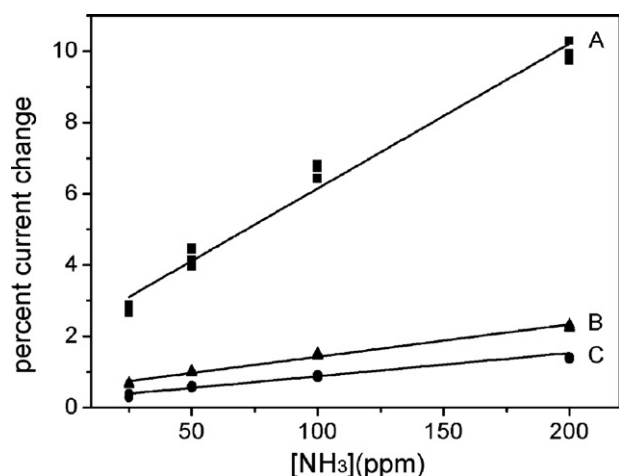


**Fig. 6.** Sensor response varies linearly with  $\text{NH}_3$  concentration of MSDI 1 (A), MSDI 2 (B) and MSDI 3 (C). The slope ( $\% \text{ppm}^{-1}$ ,  $R^2 \geq 0.98$ ) for every one may be used as a measure of sensor response.

sub-layer of 15-layer thick (ca. 25 nm deduced from XRD measurement) [42] QLS film of CuTPBPc is superior to that of MSDI 2 with a sub-layer of about 500-nm thick cast film of CuPc. The results show that structure of sub-layer film from the MSDIs has a pronounced effect on the sensing behavior of the MSDI devices. In all the MSDI devices, the  $\text{Eu}_2[\text{Pc}(15\text{C}5)_4]_2[\text{Pc}(\text{OC}_{10}\text{H}_{21})_8]$  layer is the only organic film exposed to ammonia, whereas the sub-layer plays the role of modulator of the effective charge carrier's nature, by tuning the electronic characteristics of the organic heterojunction. By means of various fabrication techniques for a highly ordered film, it is possible to select the active sub-layer with suitable characteristics for improving the top-/sub-layer interface and enhancing the performances of the MSDI-based sensors. It is worth noting that, in comparison with  $\text{LuPc}_2/\text{PTCDI}$  MSDI heterojunction-based ammonia sensor in our previous study [21], **MSDI 1 in the present case has shown higher sensor response ( $0.04\% \text{ppm}^{-1}$  vs.  $0.02\% \text{ppm}^{-1}$ ) with shorter dynamic exposure and recovery period (1 min/4 min vs. 2 min/8 min) and better stability and reproducibility evaluated from drift of current. In addition, instead of vacuum-deposited films used in top-layer of  $\text{LuPc}_2/\text{PTCDI}$  MSDI heterojunction, simpler solution-processed film is used as top-layer in this work.**

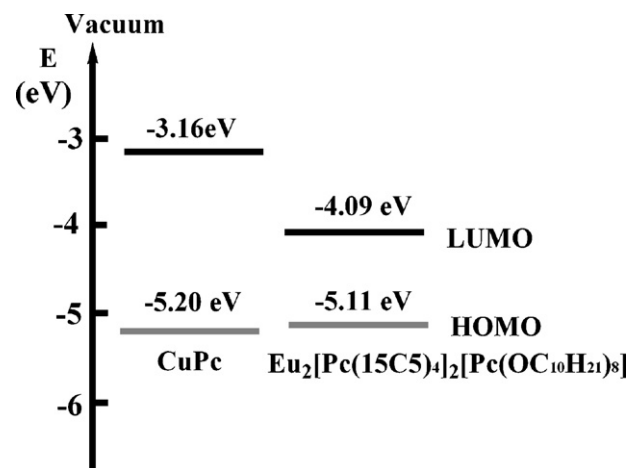


**Fig. 8.** Energy level diagram for CuPc and the  $\text{Eu}_2[\text{Pc}(15\text{C}5)_4]_2[\text{Pc}(\text{OC}_{10}\text{H}_{21})_8]$  molecules.

Since both  $\text{Eu}_2[\text{Pc}(15\text{C}5)_4]_2[\text{Pc}(\text{OC}_{10}\text{H}_{21})_8]$  and MPCs compounds are very functional materials used in organic electronics purposes due to their efficient hole transport skills [14,26], the response of individual  $\text{Eu}_2[\text{Pc}(15\text{C}5)_4]_2[\text{Pc}(\text{OC}_{10}\text{H}_{21})_8]$  QLS film and CuPc vacuum-deposited film to ammonia was determined to assess their roles as the top-layer and the sub-layer in the MSDI 1 heterojunction behavior (Fig. 7). Evidently, single component films of  $\text{Eu}_2[\text{Pc}(15\text{C}5)_4]_2[\text{Pc}(\text{OC}_{10}\text{H}_{21})_8]$  or of CuPc exhibited lower reversibility, reproducibility, response to  $\text{NH}_3$  than MSDI 1 in the same experimental condition. In agreement with the reported ammonia sensing behavior from metallophthalocyanine-based chemiresistors [7], neat CuPc film exhibits poor sensitivity to  $\text{NH}_3$  (Fig. 7a(1) and b(1)). On the opposite,  $\text{Eu}_2[\text{Pc}(15\text{C}5)_4]_2[\text{Pc}(\text{OC}_{10}\text{H}_{21})_8]$  QLS film is rather sensitive to  $\text{NH}_3$  (Fig. 7a(2) and b(2)). It is well known that the response of the chemoresistive sensors to electron-donating (reducing) gas, such as  $\text{NH}_3$ , depends on the nature of electron affinity of the molecular materials used, which in turn influences the charge transfer interaction [39]. Therefore, the schematic energy levels of CuPc and  $\text{Eu}_2[\text{Pc}(15\text{C}5)_4]_2[\text{Pc}(\text{OC}_{10}\text{H}_{21})_8]$  are shown in Fig. 8, which are accepted values cited in the literature [15,32]. It can be seen that  $\text{Eu}_2[\text{Pc}(15\text{C}5)_4]_2[\text{Pc}(\text{OC}_{10}\text{H}_{21})_8]$  accepted electrons more eas-

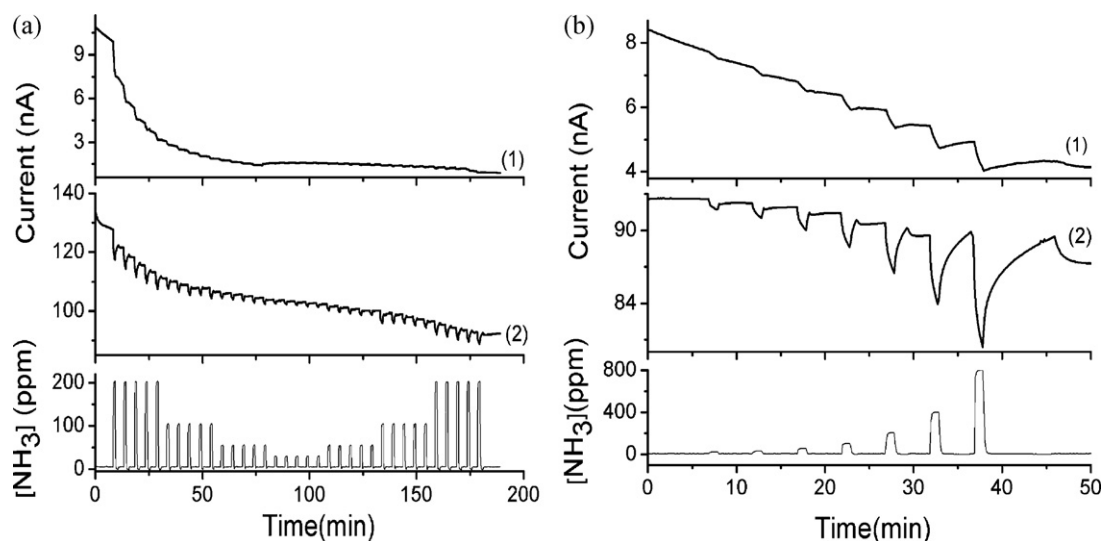


**Fig. 7.** The time-dependent current plots of CuPc vacuum-deposited film and the  $\text{Eu}_2[\text{Pc}(15\text{C}5)_4]_2[\text{Pc}(\text{OC}_{10}\text{H}_{21})_8]$  QLS film exposed to  $\text{NH}_3$  at varied concentrations in the range of (a) 50–200 ppm and (b) 15–800 ppm (exposure: 1 min, recovery: 4 min), while the bottom rectangular pulses for each current plot represent the  $\text{NH}_3$  concentration as a function of time.

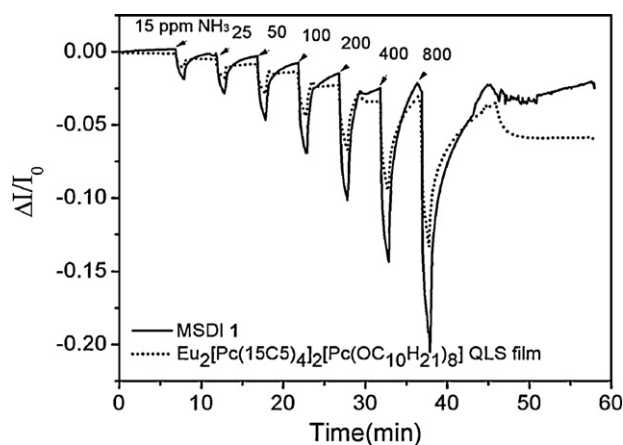


**Fig. 9.** Comparison of time-dependent relative differential current response for the  $\text{NH}_3(\text{g})$  concentrations in the range of 15–800 ppm of the MSDI **1** (solid line),  $\text{Eu}_2[\text{Pc}(15\text{C}5)_4]_2[\text{Pc}(\text{OC}_{10}\text{H}_{21})_8]$  QLS film (dotted line).

ily than CuPc due to lower LUMO (lowest unoccupied molecular orbital) energy value ( $-4.09$  eV) versus ( $-3.16$  eV). For this reason, strong electron acceptors, such as  $\text{Eu}_2[\text{Pc}(15\text{C}5)_4]_2[\text{Pc}(\text{OC}_{10}\text{H}_{21})_8]$  produce stronger responses than moderate electron acceptors, such as CuPc. On the other hand, in comparison of MSDI **1** (Fig. 5b(1)) with neat  $\text{Eu}_2[\text{Pc}(15\text{C}5)_4]_2[\text{Pc}(\text{OC}_{10}\text{H}_{21})_8]$  QLS film (Fig. 7b(2)), the response profiles upon exposure to  $\text{NH}_3(\text{g})$  in the 15–800 ppm range seemed to be similar, at a first glance, with exhibiting an apparent steady-state current response. However, by comparing the time-dependent relative differential current response of the MSDI **1** and neat  $\text{Eu}_2[\text{Pc}(15\text{C}5)_4]_2[\text{Pc}(\text{OC}_{10}\text{H}_{21})_8]$  QLS film (Fig. 9), one can see that the responses of  $\text{Eu}_2[\text{Pc}(15\text{C}5)_4]_2[\text{Pc}(\text{OC}_{10}\text{H}_{21})_8]$  QLS film (Fig. 9, dotted line) were nearly half that of MSDI **1** heterojunction (Fig. 9, solid line). In any case, as a matter of fact, MSDI **1** is more reversible, reproducible and sensitive than the  $\text{Eu}_2[\text{Pc}(15\text{C}5)_4]_2[\text{Pc}(\text{OC}_{10}\text{H}_{21})_8]$  single-layer and than the other MSDI heterojunctions with CuPc cast film or CuTTBPC QLS film as a sub-layer in present case.

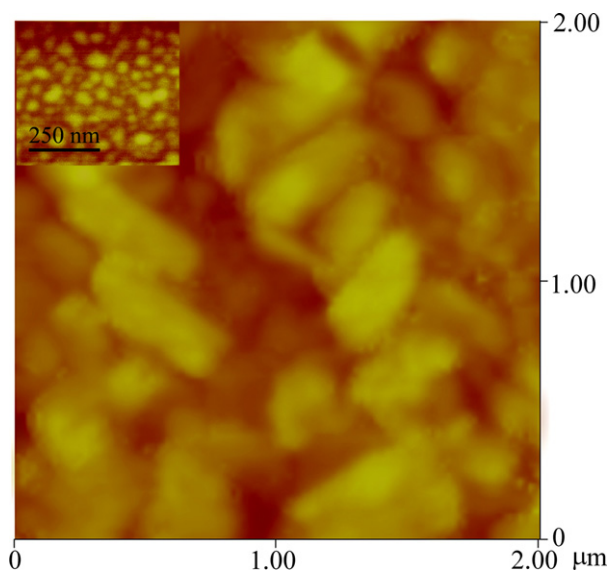


**Fig. 10.** AFM image of MSDI **1** heterojunction. The inset is of a 100-nm thick CuPc vacuum-deposited film on ITO/glass IDEs.

### 3.5. AFM observation of MSDI **1** heterojunction

The AFM image of the topology of CuPc/ $\text{Eu}_2[\text{Pc}(15\text{C}5)_4]_2[\text{Pc}(\text{OC}_{10}\text{H}_{21})_8]$  heterojunction (MSDI **1**) is shown in Fig. 10. In MSDI **1**, large crystal grains can be seen clearly, which should be mainly attributed to the contribution of top-layer,  $\text{Eu}_2[\text{Pc}(15\text{C}5)_4]_2[\text{Pc}(\text{OC}_{10}\text{H}_{21})_8]$  QLS films [22]. The inset of Fig. 10 shows the AFM image of the sub-layer of MSDI **1**, a 100-nm thick CuPc vacuum-deposited thin film. This film consists of numerous small grains covering the whole substrate. Therefore, segregated stacking between CuPc and  $\text{Eu}_2[\text{Pc}(15\text{C}5)_4]_2[\text{Pc}(\text{OC}_{10}\text{H}_{21})_8]$  molecules exists in MSDI **1** heterojunction. Obviously, it is difficult for the two-layer thin film to form an interpenetrated stacking structure, in which the CuPc thin film with numerous small grains as the matrix is filled by large grains of  $\text{Eu}_2[\text{Pc}(15\text{C}5)_4]_2[\text{Pc}(\text{OC}_{10}\text{H}_{21})_8]$ . Effective free holes or electrons reservoir (buffer effect) can be formed at the interface between CuPc sub-layer and  $\text{Eu}_2[\text{Pc}(15\text{C}5)_4]_2[\text{Pc}(\text{OC}_{10}\text{H}_{21})_8]$  top-layer when  $\text{NH}_3(\text{g})$  is involved in MSDI **1** heterojunction [20,21]. Thus, the sensing performance of MSDI **1** is highly improved.

## 4. Conclusions

A series of new MSDIs heterojunctions, MSDIs **1–3** were fabricated for chemiresistive  $\text{NH}_3$  sensing based on a novel  $\text{Eu}_2[\text{Pc}(15\text{C}5)_4]_2[\text{Pc}(\text{OC}_{10}\text{H}_{21})_8]$  QLS film as a top-layer, and vacuum-deposited and cast film of CuPc or CuTTBPC as a sub-layer. The sensing properties of the MSDIs exhibit a strong dependence on the film structure of sub-layers. By a CuPc vacuum-deposited film, with a high ordered and densely packed molecular architecture in the film matrix, as a sub-layer, MSDI **1** exhibits excellent sensitivity, reversibility and reproducibility to  $\text{NH}_3$  at varied concentrations in the range of 15–800 ppm. This provides a general method to improve sensor response of organic heterojunctions by controlling and tuning the film structure of sub-layer with appropriate fabrication techniques. The enhanced sensitivity, stability and reproducible response of the MSDI **1** heterostructure in comparison with the respective single-layer films have been obtained. A judicious combination of materials and molecular architectures has led to enhanced sensing property, in which control at the molecular level can be achieved.

## Acknowledgments

Financial support from the Burgundy region and the European Union through the FABER program is gratefully acknowledged. The authors thank the Conseil Régional de Bourgogne for a post-doctoral fellowship (Y. Chen) and for funding through the program PARI SMT 08 IME - Région Bourgogne.

## Appendix A. Supplementary data

Supplementary data associated with this article can be found, in the online version, at doi:10.1016/j.snb.2010.11.042.

## References

- [1] M. Bouvet, Radical phthalocyanines and intrinsic semiconduction, in: K.M. Kadish, R. Guilard, K. Smith (Eds.), *The Porphyrin Handbook*, vol. 19, Academic Press, Oxford, 2003, pp. 37–103.
- [2] J. Simon, P. Bassoul, *Design of Molecular Materials: Supramolecular Engineering*, Wiley, Chichester, NY, 2000.
- [3] A.W. Snow, W.R. Barger, Phthalocyanine films in chemical sensors, in: A.B.P. Lever (Ed.), *Phthalocyanines: Properties and Applications*, vol. 1, John Wiley and Sons, New York, 1989, p. 341.
- [4] M. Bouvet, G. Guillaud, A. Leroy, A. Maillard, S. Spirkovitch, F.-G. Tournilhac, Phthalocyanine-based field-effect transistor as ozone sensor, *Sens. Actuators B: Chem.* 73 (73) (2001) 63–70.

- [5] M. Bouvet, A. Leroy, J. Simon, F. Tournilhac, G. Guillaud, P. Lessnick, A. Maillard, S. Spirkovitch, M. Debliquy, A. de Haan, Detection and titration of ozone using metallophthalocyanine based field effect transistors, *Sens. Actuators B: Chem.* 72 (2001) 86–93.
- [6] M. Bouvet, Phthalocyanine-based field-effect transistors as gas sensors, *Anal. Bioanal. Chem.* 384 (2006) 366–373.
- [7] C.C. Leznoff, A.B.P. Lever (Eds.), *Phthalocyanines: Properties and Applications*, VCH Publishers Inc., New York, 1989.
- [8] M. Bora, D. Schut, M.A. Baldo, Combinatorial detection of volatile organic compounds using metal-phthalocyanine field effect transistors, *Anal. Chem.* 79 (2007) 3298–3303.
- [9] J. Simon, J.-J. Andre, *Molecular Semiconductors*, Springer-Verlag, Berlin, 1985.
- [10] V. Parra, M. Bouvet, J. Brunet, M.L. Rodriguez-Mendez, J.A. De Saja, On the effect of ammonia and wet atmospheres on the conducting properties of different lutetium bisphthalocyanine thin films, *Thin Solid Films* 516 (2008) 9012–9019.
- [11] J. Jiang, D.K.P. Ng, A decade journey in the chemistry of sandwich-type tetrapyrrolo rare earth complexes, *Acc. Chem. Res.* 42 (2009) 79–88.
- [12] J. Jiang, K. Kasuga, D.P. Arnold, in: H.S. Nalwa (Ed.), *Supramolecular Photosensitive and Electroactive Materials*, Academic Press, New York, 2001, ch. 2, pp. 113–210.
- [13] D.K.P. Ng, J. Jiang, Sandwich-type heteroleptic phthalocyaninato and porphyrinato metal complexes, *Chem. Soc. Rev.* 26 (1997) 433–442.
- [14] Y. Chen, W. Su, M. Bai, J. Jiang, X. Li, Y. Liu, L. Wang, S. Wang, High performance organic field-effect transistors based on amphiphilic tris(phthalocyaninato) rare earth triple-decker complexes, *J. Am. Chem. Soc.* 127 (2005) 15700–15701.
- [15] Y. Gao, P. Ma, Y. Chen, Y. Zhang, Y. Bian, X. Li, J. Jiang, C. Ma, Design, synthesis, characterization, and OFET properties of amphiphilic heteroleptic tris(phthalocyaninato) europium(III) complexes. The effect of crown ether hydrophilic substituents, *Inorg. Chem.* 28 (2009) 45–54.
- [16] Y. Chen, R. Li, R. Wang, P. Ma, S. Dong, Y. Gao, X. Li, J. Jiang, Effect of peripheral hydrophobic alkoxy substitution on the OFET performance of amphiphilic tris(phthalocyaninato) europium triple-decker complexes, *Langmuir* 23 (2007) 12549–12554.
- [17] R. Li, P. Ma, S. Dong, X. Zhang, Y. Chen, X. Li, J. Jiang, Synthesis, characterization, and OFET properties of amphiphilic heteroleptic tris(phthalocyaninato) europium(III) complexes with hydrophilic poly(oxyethylene) substituents, *Inorg. Chem.* 26 (2007) 11397–11404.
- [18] P. Ma, Y. Chen, N. Sheng, Y. Bian, J. Jiang, Synthesis, characterization and OFET properties of amphiphilic mixed (phthalocyaninato)(porphyrinato)europium(III) complexes, *Eur. J. Inorg. Chem.* (2009) 954–960.
- [19] M. Bouvet, V. Parra, UPMC and CNRS, FR 2007/2922310 and PCT/FR2008/001325, 2008.
- [20] V. Parra, J. Brunet, A. Pauly, M. Bouvet, Molecular semiconductor-doped insulator (MSDI) heterojunctions, an alternative transducer for gas chemosensing, *Analyst* (2009) 1776–1778.
- [21] M. Bouvet, H. Xiong, V. Parra, Molecular semiconductor-doped insulator (MSDI) heterojunctions: oligothiophene/bisphthalocyanine (LuPc<sub>2</sub>) and perylene/bisphthalocyanine as new structures for gas sensing, *Sens. Actuators B: Chem.* 145 (2010) 501–506.
- [22] Y. Chen, M. Bouvet, T. Sizun, Y. Gao, C. Plassard, E. Lesniewski, J. Jiang, Facile approaches to build ordered amphiphilic tris(phthalocyaninato) europium triple-decker complex thin films and their comparative performances in ozone sensing, *Phys. Chem. Chem. Phys.* 12 (2010) 12851–12861.
- [23] G. Guillaud, J. Simon, Transient properties of nickel phthalocyanine thin film transistors, *Chem. Phys. Lett.* 219 (1994) 123–124.
- [24] N. Padma, A. Joshi, A. Singh, S.K. Deshpande, D.K. Aswal, S.K. Gupta, J.V. Yakhmi, NO<sub>2</sub> sensors with room temperature operation and long term stability using copper phthalocyanine thin films, *Sens. Actuators B: Chem.* 143 (2009) 246–252.
- [25] K. Xiao, Y. Liu, Y. Gu, D. Zhu, Influence of the substrate temperature during deposition on film characteristics of copper phthalocyanine and field-effect transistor properties, *Appl. Phys. A* 77 (2003) 367–370.
- [26] J. Wang, H. Wang, X. Yan, H. Huang, D. Jin, J. Shi, Y. Tang, D. Yan, Heterojunction ambipolar organic transistors fabricated by a two-step vacuum-deposition process, *Adv. Funct. Mater.* 16 (2006) 824–830.
- [27] Y. Chen, H.-G. Liu, N. Pan, J. Jiang, Langmuir–Blodgett films of substituted bis(naphthalocyaninato) rare earth complexes: structure and interaction with nitrogen dioxide, *Thin Solid Films* 460 (2004) 279–285.
- [28] Y. Chen, Y. Zhang, P. Zhu, Y. Fan, Y. Bian, X. Li, J. Jiang, Arrangement of tris(phthalocyaninato) gadolinium triple-decker complexes with multi-oxyloxy groups on water surface, *J. Colloid Interface Sci.* 303 (2006) 256–263.
- [29] O. Berger, W.-J. Fischer, B. Adolphi, S. Tierbach, V. Melev, J. Schreiber, Studies on phase transformations of Cu-phthalocyanine thin films, *J. Mater. Sci.: Mater. Electron.* 11 (2003) 331–346.
- [30] Y.-L. Lee, H.-Y. Wu, C.-H. Chang, Y.-M. Yang, Substrates effects on the growth behavior of copper tetra-tert-butylphthalocyanine films studied by atomic force microscopy, *Thin Solid Films* 423 (2003) 169–177.
- [31] S. Karan, B. Mallik, Templating effects and optical characterization of copper (II) phthalocyanine nanocrystallites thin film: nanoparticles, nanoflowers, nanocabbages, and nanoribbons, *J. Phys. Chem. C* 111 (2007) 7352–7365.
- [32] W.-H. Chen, W.-Y. Ko, Y.-S. Chen, C.-Y. Cheng, C.-M. Chan, K.-J. Lin, Growth of copper phthalocyanine rods on Au plasmon electrodes through micelle disruption methods, *Langmuir* 26 (2010) 2191–2195.
- [33] M. Wojdyla, B. Derkowska, M. Rebarz, A. Bratkowski, W. Bala, Stationary and modulated absorption spectroscopy of copper phthalocyanine (CuPc) layers grown on transparent substrate, *J. Opt. A: Pure Appl. Opt.* 7 (2005) 463–466.
- [34] B.M. Hassan, H. Li, N.B. McKeown, The control of molecular self-association in spin-coated films of substituted phthalocyanines, *J. Mater. Chem.* 10 (2000) 39–45.
- [35] R.A. Hatton, N.P. Blanchard, V. Stolojan, A.J. Miller, S.R.P. Silva, Nanostructured copper phthalocyanine-sensitized multiwall carbon nanotube films, *Langmuir* 23 (2007) 6424–6430.
- [36] G. Maggioni, A. Quaranta, S. Carturan, A. Patelli, M. Tonezzer, R. Ceccato, G.D. Mea, Deposition of copper phthalocyanine films by glow-discharge-induced sublimation, *Chem. Mater.* 17 (2005) 1895–1904.
- [37] C.L. Donley, W. Xia, B.A. Minch, R.A.P. Zangmeister, A.S. Drager, K. Nebesny, D.F. O'Brien, N.R. Armstrong, Thin films of polymerized rodlike phthalocyanine aggregates, *Langmuir* 19 (2003) 6512–6522.
- [38] C.J. Liu, J.J. Shih, Y.H. Ju, Surface morphology and gas sensing characteristics of nickel phthalocyanine thin films, *Sens. Actuators B: Chem.* 99 (2004) 344–349.
- [39] B. Schöllhorn, J.P. Germain, A. Pauly, C. Maleysson, J.P. Blanc, Influence of peripheral electron-withdrawing substituents on the conductivity of zinc phthalocyanine in the presence of gases. Part 1. Reducing gases, *Thin Solid Films* 326 (1998) 245–250.
- [40] I. Lähdesmäki, W.W. Kubiak, A. Lewenstam, A. Ivaska, Interference in a polypyrrole-based amperometric ammonia sensor, *Talanta* 52 (2000) 269–275.
- [41] F.I. Bohrer, A. Sharoni, C. Colesniuc, J. Park, I.K. Schuller, A.C. Kummel, W.C. Trogler, Gas sensing mechanism in chemiresistive cobalt and metal-free phthalocyanine thin films, *J. Am. Chem. Soc.* 129 (2007) 5640–5646.
- [42] G.W. Miller, A. Sharoni, G. Liu, C.N. Colesniuc, B. Fruhberger, I.K. Schuller, Quantitative structure analysis of organic thin film: an X-ray diffraction study, *Phys. Rev. B* 72 (2005) 104113.

## Biographies

**Yanli Chen** received her MS in 2003 and PhD in 2006, both in chemistry from the Shandong University (China). She spent one year in France as a post-doctoral fellow in the research group of Prof. Marcel Bouvet, at the University of Bourgogne (Dijon, France). She is currently Professor of Chemistry at the University of Jinan (China). Her research interest focuses on the ordered molecular self-assembly, manipulation of functional molecular materials with large conjugated electronic molecular structure for molecular devices, and the investigation of their FET and gas sensing properties.

**Prof. Marcel Bouvet** obtained his PhD from the University Pierre and Marie Curie (UPMC), in 1992 on electrical properties of phthalocyanines. He has been working mainly at the E.S.P.C.I. (Paris), as associate professor, but also at the UPMC (Paris), and at the University of Connecticut (USA). He got a full professor position at the Université de Bourgogne (Dijon), in 2008. His research interests are in the field of molecular materials-based devices, among them sensors.

**Thibaut Sizun** was born in 1981. He obtained a Bachelor of Science and a Master from the Université de Bretagne Occidentale (Brest, France). He is currently preparing his PhD under the supervision of Prof. M. Bouvet on phthalocyanine-based gas sensors.

**Guillaume Barochi** was born in 1985. He obtained a Bachelor of Science and a Master from the Université de Bourgogne (Dijon, France) in 2009. He is currently preparing his PhD under the supervision of Prof. M. Bouvet and Dr. J. Rossignol on new transducers for chemical sensors.

**Jérôme Rossignol** was born in 1975. He obtained his PhD from the University Blaise Pascal (Clermont-Ferrand, France) in 2001 in physics plasma on theory and simulation of physical phenomena of cathodic arcs. He has been working for two years at the Humboldt University in Berlin (Germany) as a post-doctoral fellow. He is currently associate professor in electronics at the Université de Bourgogne (Dijon, France). His research activities are in the fields of microwave transduction and physics of plasmas.

**Eric Lesniewska** obtained his PhD from the University de Bourgogne (Dijon, France) on near field microscopies applied to biological species and materials observation. He is currently professor at the University of Bourgogne (Dijon, France). His research interests are in the field of nanbiosciences and the development of new nanoproboscopes or biosensors.